18
Cell Mechanics on Surfaces

Jessica H. Wen[1)], *Hermes Taylor-Weiner, Alexander Fuhrmann, and Adam J. Engler*

18.1
Introduction

Cells have the amazing ability not only to sense how stiff their surrounding is but also to physically respond to changes in stiffness. Examples of this cellular response include migration following a stiffness gradient [1–3] and differentiation toward different lineages depending on the substrate stiffness [4]. Historically, cell culture *in vitro* is performed in a Petri dish made of tissue culture plastic, a material that is extremely stiff compared to native tissue stiffness *in vivo*. Only in recent years has it been shown that the use of tissue culture plastic neglects the significant influence substrate mechanics or elasticity (more commonly referred to as *stiffness* – albeit incorrectly – in a biological context) can have on cell behavior. This chapter provides information on how to fabricate more *in vivo*-like materials by carefully controlling substrate stiffness. Before doing so, the terms *stiffness* and *elasticity* need to be defined.

18.2
What Is Elasticity and Stiffness?

Elasticity is a physical property of materials that describes their ability to undergo deformation and return to their original shape after a previously applied stress or deformation is released; it may be described as linear or nonlinear. An ideal, fully elastic material exhibits linear elasticity where there is a linear relationship between the amount of deformation an object undergoes and the force that had to be placed on the surface of that material to cause the deformation. Perhaps the simplest illustration of linear elasticity in physics is a spring. In 1678, Robert Hooke proposed the linear relationship of force and displacement in an ideal spring: $F = kx$, where F denotes the force, k is the spring constant, and x is displacement of the spring. This physical law, commonly known as *Hooke's law*,

1) Authors Jessica H. Wen, Hermes Taylor-Weiner, and Alexander Fuhrmann contributed equally.

Biomaterials Surface Science, First Edition.
Edited by Andreas Taubert, João F. Mano, and J. Carlos Rodríguez-Cabello.

describes a constant relationship between force and displacement. A material exhibiting nonlinear elasticity, or in this case a nonlinear spring, would thus have a varying relationship between F and x. Most real materials, especially biological materials, exhibit a combination of linear and nonlinear elastic behavior.

When an external force is applied to a material, the material is internally compressed (stressed) and subsequently deforms (strains). In mechanics, the intrinsic property of a linear elastic material is called Young's modulus (E), which describes the ratio of uniaxial stress – the amount of force applied through a cross-sectional area – divided by the uniaxial strain – the normalized deformation of the material, for example, the change in length divided by the original length of the material (Figure 18.1a inset). The material's *Young's modulus* is thus defined as the slope of the stress versus strain curve and is measured in pascal (Pa) or newton per square meter ($N\,m^{-2}$). In the human body, tissue may be as stiff as several gigapascal (bone) or as soft as only few kilo pascals (fat) (Figure 18.1b). However, most biological materials have a "toe" region, where the tissue is nonlinearly elastic and then appears linear over a range of small strains before transitioning into a nonlinear regime at larger strains (Figure 18.1a). Nonlinear elasticity is described by finite strain theory, and in most cases this transition occurs when the external stress causes plastic deformation or yielding, an irreversible change of shape of the material. While this is just one example of nonlinear elasticity among many other types, we will limit the description here to biomaterials.

A commonly observed effect of nonlinear elasticity in biological networks is strain stiffening. For example, cross-linked fibrin scaffolds formed after an injury

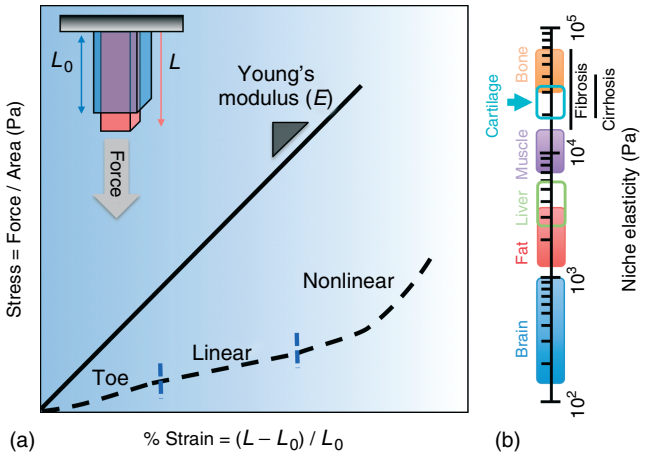

Figure 18.1 Stress–strain behavior and elasticity in tissues: (a) Diagram of Newtonian (ideal) behavior of a linearly elastic material (solid line). A typical stress–strain curve for a tissue (dashed line) has both linear and nonlinear regimes corresponding to cells and matrix within the tissue differentially undergoing strain. An illustration of how a material is put under stress and strain to make this measurement is inset. (b) Young's moduli for the biological materials indicated (colors) as well as how diseases can alter moduli from overexpression of matrix or other mechanisms (black).

to prevent bleeding render the tissue stiffer than prior to the clot. After strain stiffening, materials have an increased modulus with increased load. Because biological networks such as extracellular matrix (ECM) are composed of long protein chains, the onset of strain stiffening can occur suddenly and irreversibly. While these matrix networks can move and deform freely under small strains, the force needed to further deform the network increases drastically once the connecting proteins within the network are maximally unfolded and then begin to stretch. Another important example of nonlinear elasticity is anisotropy, or exhibiting directionally dependent properties, and an often cited example is cortical bone: its axial and transverse moduli are 23 and 17 GPa, respectively [5].

The complex, fibrous, and entangled characteristic of many network-based biological materials and biomaterials is responsible for deviation from the linear elasticity theory and prevents these materials from being described as perfectly elastic, even at small strains. These networks, found in almost every biological material including cells, are well hydrated and the transport of water and other solvents during compression or tension can modulate how the rate of applied stress influences the strain response, that is, viscoelasticity, which is discussed at length later in this section of the chapter. While the initial shape may be restored after the release of previously applied stress meeting the first criterion of linear elasticity, strain becomes dependent on time, fluid viscosity, and network pore size. A viscoelastic material, which describes most biological tissues, can have an elastic region on the stress–strain curve, and are thus approximated as elastic at certain stresses and strains without being truly elastic. An in-depth discussion of the biomechanical properties of biological materials can be found in Fung's work on biomechanics [6].

Young's modulus is a measure for the strain response due to a normal stress applied perpendicular to the surface, a simple characterization for completely elastic materials. However, because many biomaterials are viscoelastic, it is important to also define the shear modulus (G), a measure for the strain response due to a shear stress applied parallel to the surface. The shear modulus is related to Young's modulus via the Poisson's ratio (ν) such that

$$E = 2\,G(1+\nu) \tag{18.1}$$

Poisson's ratio is the ratio of the contraction or transverse strain applied perpendicular to the load, to the resulting extension or axial strain parallel to the load [6]. Perfectly incompressible materials maintain their volume under stress because their axial elongation is perfectly balanced by an inward lateral strain resulting in a Poisson's ratio of 0.5 (e.g., rubber [7]). Perfectly compressible materials do not maintain their volume under stress and have a Poisson's ratio of 0 (e.g., cork [8]). However, most real materials display both compressible and incompressible behavior creating biomaterials with Poisson's ratios ranging between 0 and 0.5.[2] It must be noted here that the relationships between E, G, and ν may not apply for

2) Some materials can have negative Poisson's ratios down to −1. However, a discussion of this would go beyond the scope of this chapter.

nonlinear elastic materials. As a result, it is important to keep this in mind when choosing or comparing experimental methods to measure stiffness.

This chapter first (i) focuses on methods of measuring substrate elasticity, that is, biomechanics, then (ii) provides a discussion of how biomaterials may be fabricated and tailored to a desired stiffness to drive cell behavior, and finally (iii) describes the mechanical interactions of cells with their surroundings, that is, mechanobiology [9]. However, before beginning these discussions, it is important to place these concepts in the context of a cell. First, cells move and interact with their surroundings rather slowly (with the exception of e.g., contracting muscle cells), and given the time scale of this interaction, the elastic component of most viscoelastic biomaterials should dominate. Consequently in most cases, the elastic component of stiffness has been measured while viscous contributions are not described. Second, cells interact and ''feel'' their surrounds at the micrometer length scale. Should heterogeneity exist in a material at that length scale which is not well represented in bulk measurements, cell behavior may be less predictable. Thus, the elasticity measure method needs to be done with length scale in mind. Stiffness of a material may vary significantly if measured on a microscopic level compared to a macroscopic level, as has been shown for polyvinylpyrrolidone [10].

18.3 Measuring and Quantifying Stiffness

Mechanical properties of solid elastic materials can be easily measured via tensile or compression testing, but as previously mentioned, most biological materials and biomaterials used in cell culture are viscoelastic. The most common set of methods used to measure the relationship between deformations and resultant stresses of fluid-like materials is rheometry. A rheometer measures the macroscopic shear properties of viscoelastic materials by applying a force parallel to the material's surface, rather than perpendicular, as with tensile or compressive loading. For linearly elastic materials, macroscopic properties directly translate to microscopic properties, which is an important point in continuum mechanics [6]. While the properties determined using a rheometer can be useful when describing different surfaces for cell culture, a more complete description of the surface's mechanics is perhaps more useful as most biomaterials display nonlinear elasticity. In the following discussion, we give a brief overview of the methods that may be used to create a more complete material description and the mechanical parameters used to accomplish this, most notably shear moduli (G', G''), Young's modulus (E), and bulk modulus (K). For materials that exhibit linear elasticity, well-defined relationships have been established between the individual moduli. Consequently, it is sufficient to measure just one modulus, which can be used to derive the others. G' is commonly measured by a rheometer, which spins a plate inside the liquid of interest creating a shear force. E is commonly obtained by measuring the strain response to a linearly applied stress. There is currently no commonly used technique to measure K as stress needs to be applied and measured in all

three dimensions simultaneously. The following section of this chapter describes methods of how to measure the moduli of both linearly elastic and nonlinearly elastic materials.

18.3.1 Measuring Linearly Elastic Properties

A rheometer (Figure 18.2a, [left] shown with a cone-and-plate configuration) is the most commonly used device to measure shear modulus (G'). Although rheometers are traditionally used in material science to describe properties of viscous fluids, they have been also utilized in biomaterial science for viscoelastic materials such as hydrogels. While there are many different types of rheometers that can be used to measure fluids properties, soft materials are usually probed by a shear rheometer, a device that applies shear stress by rotating a disc or cone that is in contact with the material on one side while on the opposing side the material is in contact with a fixed, flat plate. The velocity of the disc measured in rotations per minute (rpm) has to be adjusted to the viscosity of the sample as detected by the force felt by the opposing, fixed plate. The stiffer, and thus more viscous, the sample is, the lower the rpm of the probe. For stiffer materials, the probe can be rotated back and forth. Rheometers are also used to measure viscous responses or loss moduli (G'') in materials; this discussion continues in the nonlinear elasticity section.

While a rheometer applies a force parallel to the material's surface to measure the shear modulus in complex viscous fluids and solid materials, Young's modulus of a solid material can be more directly accessed by an indentation perpendicular to the surface or extension of one end of the material relative to the other fixed end. Most simply put, a stress is applied perpendicular to the surface of the material, and the strain response of the material as a result of the applied stress is measured. *Young's modulus* (E) is defined as stress (σ) divided by strain (ε). Stress σ is F/A_0, where F is the magnitude of force applied, and A_0 is the initial cross-sectional area of the samples. Strain, ε, is most often described as the change in length divided by the original length or $\Delta L/L_0$. For macroscopic materials, E can easily be obtained by measuring the applied load and deformation during compression loading. This is commonly done in compression testing where the load is being applied by a macroscopic plate that covers the entire sample resulting in a single E measurement for each sample. However, if the microscopic properties or stiffness heterogeneity of a sample are of interest, as is sometimes the case in hydrogels [10], the contact area of the applied load to the sample must be extremely small – from centimeters down to nanometers. This type of microscopic indentation perpendicular to the surface is typically achieved by pushing a probe or indenter with a well-defined shape directly into the sample [13], and it is most often performed using an atomic force microscope (AFM; Figure 18.2a, right). On recording the load and displacement generating a load–indentation curve, Young's modulus can be calculated using the known contact area of the indenter, typically a sphere or a pyramid, and the sample.

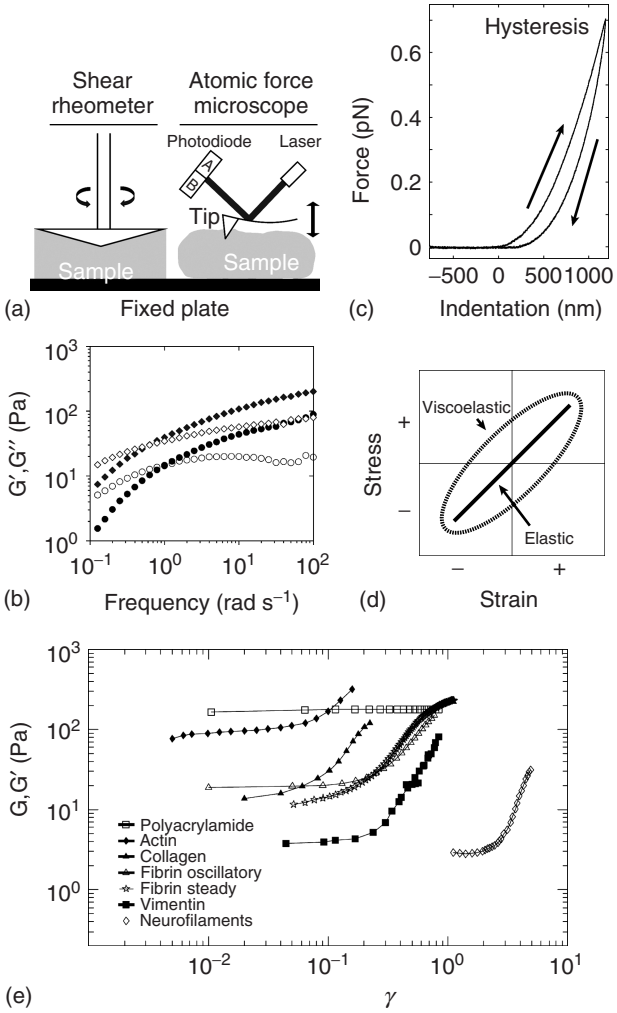

Figure 18.2 Measurement methods for surface mechanics. (a) Illustration of a cone-and-plate shear rheometer (left) and an atomic force microscope (AFM)-based indentation (right). (b) Oscillatory frequency sweeps from cone-and-plate rheometry on polyethylene glycol hydrogels of different mixing ratios indicated by the circles and diamonds. Storage moduli (G') are indicated by filled data points while loss moduli (G'') are indicated by open data points. Reproduced from Lu *et al*. [11]. (c) Schematic of a hysteresis effect in a viscoelastic material with arrows to indicate indentation and retraction of the indenting probe. (d) General stress–strain relationship in an elastic and viscoelastic material. (e) Data shown are storage moduli (G) at 10 rad s^{-1} over a range of dimensionless strain γ for F-actin, fibrin, collagen, vimentin and polyacrylamide, and shear modulus (G) for fibrin and neurofilaments, plotted over the same a range of dimensionless strain γ. Linear behavior indicates elastic responses. Reprinted from Storm *et al*. [12].

In addition to indenter probe size, indentation depth is important to control and should be limited. That way, the strain field should decay before reaching the underlying rigid support to which the material is bound [14]. If this does not occur, the indenter will essentially ''feel'' the underlying substrate. Limiting the indentation depth is also important because it ensures that the contact area will always be known; should the indentation geometry change, it needs to be accounted for by correction terms in the analysis methods. Most often, these correction terms modify these methods by multiplying them with a Taylor series expansion in material thickness [15]. A key advantage of the indentation methods is that the size of the indenter can be scaled down to nanometers, and with the small indenters, indentation depth can be significantly reduced, thus ensuring accurate detection. This is most important when measuring the mechanics of thin cells cultured on a thick, rigid substrate, such as tissue culture plastic. With nanometer indentations, the indenter avoids ''feeling'' the underlying stiff plastic substrate. Minimizing indentation depth for biological materials is also critical because at larger strains, these materials may exhibit nonlinear elasticity; mimicking the relevant forces and length scales is crucial.

Knowing the considerations for making small mechanical measurements by indentation, we now more formally introduce the technique of AFM indentation. AFM is a technique originally designed for scanning surfaces in nanometer resolution, but also has excellent force resolution (Figure 18.2a, right). The indenter, usually a triangular-pyramidal or spherical tip, is attached to a cantilever beam. When the indenter approaches the substrate surface controlled by piezoelectronics, the cantilever bends following Hooke's law, that is, the force acting on the sample can be calculated by measuring the deflection of a laser spot reflecting from the top of the cantilever and multiplying that by the spring constant of the cantilever. The depth of indentation, that is, how far the probe pushes into the sample, can be obtained from the force–distance curve. Knowing the geometry of the indenter and indentation depth, one can now compute the contact area of the indenter probe and sample. The force–indentation curve can now be fitted with the following equation:

$$F(\delta) = \lambda \delta^{\beta} \tag{18.2}$$

where F denotes the force of indentation and δ denotes the depth of indentation [16]. The term λ and the exponent β depend on the geometry of the indenter probe; a table of different values for λ and β can be found in Lin and coworkers [16].

Besides simply indenting the sample surface in the z-direction with an AFM to determine elasticity at a given point, spatial homogeneity of a material can also be obtained using piezos actuators in the x and y planes to move the sample in a precise manner. The heterogeneity of a sample can be assessed anywhere between nanometer and millimeter resolution using AFM depending on the indenter size and how regular the user makes use of an indentation grid when examining the sample's surface.

18.3.2 Measuring Nonlinearly Elastic Properties

Methods to measure the moduli of nonlinear elastic materials typically utilize the same general tools and concepts as those for linear elastic materials but with modifications to the modes of operation. The vast majority of biomaterials display nonlinear elastic behavior because of viscoelasticity, and can be described by several constitutive models including the standard linear solid, Maxwell, and Kelvin–Voigt models. These constitutive models require specific material properties including moduli and relaxation constants that must be previously measured. For a more complete discussion of these viscoelastic models, please see discussions from Fung [6]. The strain response of a viscoelastic material is dependent on the rate of the applied stress because the viscous portion of the material relaxes or flows with time. To account for this, the rheological description of such materials is frequency dependent: by applying an oscillatory (sinusoidal) stress in shear or compression, slower or faster, more fluid-like or solid-like moduli can be determined, respectively. The elastic or solid-like portion is described by the storage modulus (G'), a measure of energy stored, and is usually higher at higher frequencies for biological materials and biomaterials. The viscous portion is described by the loss modulus (G''), a measure of energy dissipated because of friction or flow of the material. The dynamic modulus used to describe viscoelastic materials is a combination of both the storage and loss moduli with all three being frequency dependent. Hydrogels, such as the poly(ethylene glycol) (PEG) system shown in Figure 18.2b [11], can be easily measured using rheology and show a solid to liquid transition when $G' > G''$, typically around 1 Hz. In the context of the cell, materials should appear solid-like as individual actomyosin contractions occur at frequencies well above the transition point. Within a cell, the creep response, stress relaxation response, and the bulk modulus all follow a power-law behavior, which is more commonly attributed to the behavior of soft glassy materials [17]. What drives this response is likely the macroscopic arrangement of stress fibers and actomyosin cross-bridging cycles [18]. Aside from the cells themselves, these frequency behaviors in shear and loss moduli should be maintained.

A viscoelastic material also can exhibit hysteresis (energy loss in a stress–strain curve), stress relaxation (constant strain causes decreasing stress), and creep (constant stress causes increasing strain). As shown in Figure 18.2c (top), material indentation is often an easy way to observe hysteresis. For linear materials, indentation and retraction curves should overlap, but in a nonlinearly elastic or viscoelastic material, the two curves will often not overlap. Subsequent indentations can also shift as residual stress builds in the material over multiple indentation cycles. Besides viscoelasticity, the other major contributor to nonlinear elasticity of biological materials is strain stiffening. As the stiffness increases with increasing strain, oscillation amplitude of the cone when using a rheometer, or the indentation depth when using a nanoindenter or AFM can be increased. Resulting elastic moduli are then reported on the basis of their dependence on strain.

Overall, measurement methods essentially cycle through four different states, and depending on the shape of the material's response data, one can predict more elastic, viscous, or viscoelastic behavior. Elastic materials, when loaded normal to their surface in compression or tension will compress (''negative'' strain) or will expand (''positive'' strain) (Figure 18.2d). Viscoelastic samples will have stress and strain responses out of phase, with the general relationship in the material being:

$$\sigma(\omega t) = G'\gamma sin(\omega t) + G''\gamma cos(\omega t) \tag{18.3}$$

where γ is strain, ω is the phase lag, and t is time. Thus, at some time when the stress is at a maximum, strain is out of phase and is not yet at a maximum. This is often shown in the form of a Lissajou plot where the phase lag is illustrated. Additional discussion of these plots and viscoelastic biomaterial characterization is provided by Ferry [19] and Fung [6]. For the simple purposes of describing biomaterials, current convention dictates reporting shear and loss moduli. There are a variety of material behaviors in biological materials and biomaterials, notably strain-stiffening as shown from the nonlinear, positive slopes for data in Figure 18.2e. We next attempt to introduce those substrates.

18.4
Controlling Substrate Stiffness

The first two-dimensional tissue culture experiments, conducted by Wilhelm Roux in 1885, grew the medullary plate of embryonic chickens on glass plates. Two years later, Julius Petri created the first glass Petri dish, and plastic (usually polystyrene) versions of his original design have been used for cell culture ever since. It is not hard to see why glass and hard plastic substrates are popular; they provide an optically clear, flat surface where certain cell types spread and divide rapidly. However, these substrates are super-physiologically stiff (10^9 Pa) and many cellular functions, including proliferation [20], differentiation [4], apoptosis [20], and migration [3], change when cells interact with more physiologically stiff substrates (10–10^5 Pa) (Figure 18.1b) [21]. These observations highlight the importance of considering substrate stiffness when engineering materials for biological applications.

18.4.1
Material Properties That Determine Stiffness

The modulus of a polymer is governed by four molecular properties: concentration; pore size; network order, or crystallinity, or chain length (molecular weight); and cross-linking (Figure 18.3). Each of the scaffolds mentioned below manipulates one or more of these properties to control stiffness. Materials with long polymer chains are stiffer because of increased chain entanglement and crystallinity. Increasing the concentration of polymer or decreasing the pore size raises a material's modulus by lowering the void volume. Chemical cross-links prevent polymer chains from sliding relative to one another, making the material more resistant to

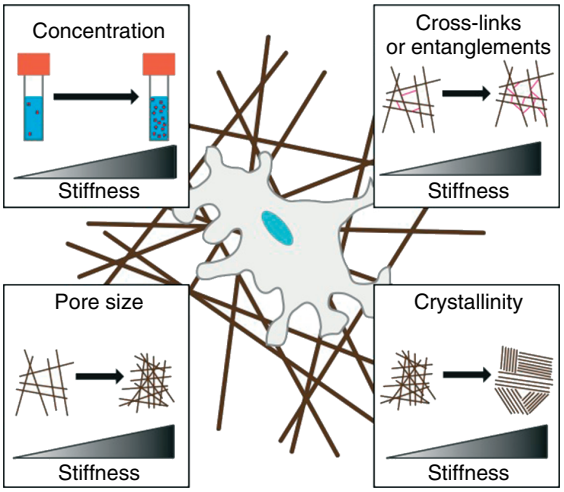

Figure 18.3 Controlling matrix stiffness. Illustration of several factors that can easily modify matrix stiffness.

deformation [22]. It is these properties and their resulting structural organization that dictate material properties, including stiffness [23]. Whether one uses an amorphous hydrogel or an electrospun fiber mesh, structural organization can create additional properties, such as anisotropy. For example, fiber orientation and thickness can change the effective stiffness of a substrate [24]. A single fiber is inherently stiffest in the fiber direction and weakest in the perpendicular direction [24]. If a fibrous material is randomly oriented, the material will exhibit the same mechanical properties in every direction (isotropic). On the other hand, local fiber organization, for example, alignment, can cause cells to sense a directionally dependent or anisotropic increase in stiffness and elongate in the fiber direction [25]. By exerting small forces onto a substrate, cells create deformation fields that decay with distance from the cell in a manner that depends on the magnitude of the force and the material's mechanical properties. If the deformation field crosses a material interface (e.g., polymer to glass) or if the material is sufficiently thin such that the underlying support is felt, for example, 2 μm for a material with an elastic modulus of 8 kPa [14], then the mechanical properties of the neighboring material will change the effective stiffness sensed by the cell. Therefore, material choice, its structure, and fabrication can all influence cell behavior, and thus an in-depth look at biological materials and biomaterials is warranted.

18.5 Naturally Derived Scaffolds

A variety of naturally derived materials have been used as cell culture substrates [26–31] and a body of literature for controlling stiffness has grown around many of

them [32, 33]. Rather than try to describe them all, we focus on three representative and popular materials: collagen, hyaluronic acid (HA), and cell-derived ECMs.

18.5.1 Collagen Type I

Representative of ECM protein hydrogels, collagen readily supports cell attachment and spontaneously gels at temperatures suitable for cell culture [29, 34]. Although at least 29 naturally occurring types of collagen have been identified [35], most collagen gels are composed of the fibrillar collagens – type I, II, III, V, XI, XXIV, and XXVII–which account for approximately 90% of all of the collagen in the body by mass [29]. At a molecular level, fibrillar collagens are formed by three chains wound together in a triple helix. Each chain type is encoded by a specific gene, but these can often be repeated; for example, two α1 and one α2 chains comprise type I collagen. This structure is almost exactly conserved in vertebrates as well as chordates [36]. The chain flexibility necessary to form the helix arises from the protein's repeated amino acid sequence, Gly-Pro-X, where X can be any amino acid residue. This sequence also gives rise to sites for natural cross-linking, which enables tissues to change collagen mechanics as mentioned here.

Collagen assembly and mechanics are tightly regulated *in vivo*. Collagen is produced as immature procollagen by cells and secreted into the ECM, where the alpha chains undergo enzymatic removal of N- and C-terminal peptide sequences [29]. Mature collagen proteins self-assemble into insoluble fibrils that can be chemically cross-linked through glycation [37], mineralization [38], and enzymatic alterations [39]. These modifications can have pathological significance; for example, lysyl oxidase catalyzed collagen cross-linking maintains a malignant phenotype in breast cancer [40]. The mechanical properties of many tissues are determined, in large part, by their collagen concentration, its organization, and its degree of cross-linking. Conversely, collagen gels *in vitro* are fibrillar (Figure 18.4a) and often formed via noncovalent interactions, for example, chain entanglement, which can be induced by raising the solution temperature (e.g., 37 °C), raising pH, or increasing the collagen concentration [34]. Importantly, changing collagen pH and concentration also alters the chain density and pore size of the resulting gel, affecting its stiffness [41]. Using only these variables, it is possible to create gels *in vitro* with moduli on the order of hundreds of pascals, although many tissues rich in collagen are much stiffer *in vivo*. (Figure 18.1b) [21]. To increase stiffness even further *in vitro*, chemical cross-links can be formed between the collagen molecules using ribose sugar [37], genipin (a fruit extract) [42], and glutaraldehyde [43] among others. Even stiffer gels can be created by doping in a second polymerizing solution, creating a composite material or interpenetrating network (e.g., agarose/collagen gel [44]). Using these techniques, collagen gels with Young's moduli in the range of 10^1–10^3 Pa may be achieved [21, 37, 42–44].

There are several advantages to using collagen gels for cell mechanics experiments. The gels are bioactive and three-dimensional, allowing cells to bind,

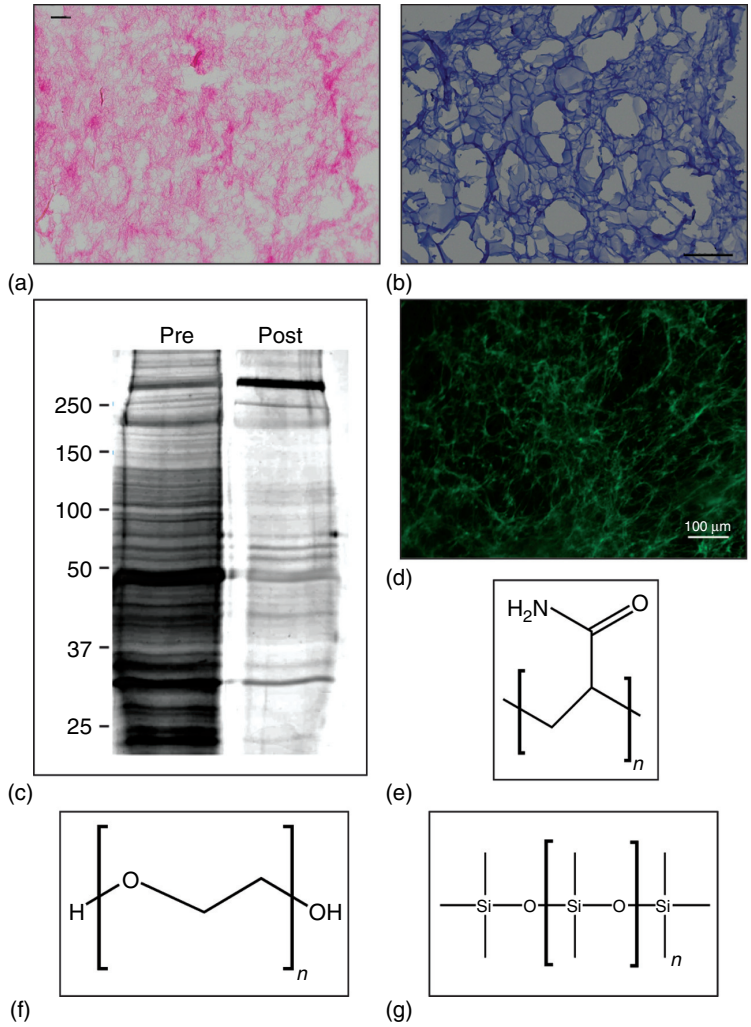

Figure 18.4 Cell culture substrates with controllable stiffness. Naturally derived scaffolds for cell culture include gels composed of (a) collagen type I (stained with picrosirius red) and (b) hyaluronic acid (stained with hematoxylin). (c) The cellular components (pre) can be removed from the cell-derived extracellular matrix (post) resulting in (d) a decellularized fibrillar matrix (immunostained fibronectin colored green). Synthetic hydrogels used for cell culture include (e) polyacrylamide, (f) polyethylene glycol, and (g) polydimethylsiloxane.

remodel, and migrate through an environment that closely approximates a native ECM. Gel formation is simple and the materials required are commercially available. The major limitations include the relatively small stiffness range that can be easily achieved and the difficulty of decoupling matrix chemistry from mechanics, that is, changing concentration to increase stiffness, also adds more

ligand and makes pore sizes smaller, thus restricting cell movement [45]. Nevertheless, collagen gels are an important and widely used substrate for probing cell mechanics.

18.5.2 Hyaluronic Acid

Glycosaminoglycans (GAGs) are linear polysaccharides that are formed from linked disaccharide units. The sugar chains may be many thousands of repeats long, resulting in molecular weights in the mega-Daltons, and depending on the type of GAG it may carry a large negative charge [46]. In tissues, GAGs are synthesized by cells and can be linked to insoluble ECM proteins, such as collagen. HA, a GAG abundant in the fluid lubricant of joints and the ECM of many tissues, is commonly studied *in vitro* because of its mechanical properties. HA is unique among GAGs because the two sugars that make up its disaccharide repeat unit (*N*-acetylglucosamine and glucuronic acid) do not contain negatively charged sulfate groups. Consequently, the molecule exhibits a lower charge density than other GAGs at physiological pH. Instead, HA contains an abundance of amide, hydroxyl, and carboxylate side groups that make the molecule hydrophilic, soluble in aqueous solutions, and easily modifiable to make hydrogels with tailored responses [47]. Cell types that express CD44, an extracellular membrane bound protein, are able to bind directly to HA and use it as a substrate for attachment, migration, and proliferation [48].

Unlike type I collagen, solutions of unmodified HA cannot easily be converted from a liquid to a gel. The hydrophilic side groups make chain entanglement unfavorable and keep HA soluble under physiological conditions. To form a gel, the reactive side groups on HA must be chemically modified such that cross-links can form between the chains. This has been accomplished using several different methods [47], with thiolation [49] and methacrylation [50] being the most common modifications. Using similar techniques, HA can also be linked to bioactive peptides [51] or entire proteins [52] to enhance integrin-mediated attachment or elicit a specific cellular response. These modifications result in changing the mechanical stiffness of HA hydrogels, but such changes depend on the polymer concentration and the number of cross-links [53]. The amount of cross-linking is limited by the degree of modification to the HA; more completely modified HA gels are usually stiffer. Most polymerization schemes result in hierarchical HA materials (Figure 18.4b) with Young's moduli that are on the order of $10^1 - 10^4$ Pa [47, 50]. Hydrogels composed of modified HA have also been engineered to undergo controlled stiffening or softening by introducing degradable cross-links that are light sensitive [54] or by forming those cross-links gradually over time [55].

The principle advantage of using HA gels to study cell mechanics involves the chemical modifications that can be added to the sugar backbone. Many modifications available are well characterized and allow for careful control of the gel's chemical and mechanical properties, both statically and dynamically. However, these hydrogels should normally also be modified with an adhesive protein to encourage integrin-mediated adhesion; CD44 negative cells will not

adhere to HA, and for those that do, CD44 is loosely cytoskeletally linked at best [48]. Moreover, HA hydrogels may have a limited stiffness range depending on the type of modification.

18.5.3 Cell-Derived Extracellular Matrix

The best approximation for a native ECM that one can obtain *in vitro* is decellularized cell-derived matrix, which can be obtained via detergent solubilization methods that allow the matrix to remain intact; this process has become well established both for matrices assembled *in vitro* [56] by cells and *in vivo* by tissues [31]. The ECMs produced by different cell types are basement membranes, that is, sheet-like structures composed of laminins, collagens, and entactins [57], and interstitial matrices. The latter are three-dimensional web-like structures made up of small protein fibers (less than 1 μm in diameter) noncovalently linked together [23]. The interstitial matrix fills the space between neighboring cells and gives tissues their structural integrity. Although the composition varies dramatically from one tissue type to another, fibronectin, collagens, and GAGs are common components of interstitial matrices [29]. Just like native extracellular environments, *in vitro* cell-derived matrices are dynamic and complex. The composition and structure of the matrix are cell-type and culture-condition specific, sometimes making reproducibility difficult. Moreover, ECMs undergo constant cell-mediated remodeling during culture and can sequester soluble growth factors and cytokines [58]. These soluble factors often remain bound throughout the decellularization process and affect the behavior of cells reseeded onto the decellularized scaffold [59].

The most common commercially available cell-derived ECM is Matrigel, a self-assembling basement membrane produced by an immortalized mouse sarcoma cell line [57]. Matrigel can be formed into thin films or thick gels for cell culture by simply raising the temperature of the solution to 37 °C. Reconstituted, lyophilized matrix derived from specific tissues has also become an interesting off-shoot of the work from Ott and coworkers [31, 60]. These reconstituted networks have highly tunable substrate surface properties, but may not have the same bioactivity as natural tissue-bound matrix. Fibrillar, decellularized matrices, on the other hand, can be created from any cell type that produces sufficient ECM *in vitro* and thus maintains its structure and activity during decellularization. To produce this matrix, the cells of interest, most commonly fibroblasts as they produce significant amounts of matrices, are grown on a plastic substrate under confluent conditions that promote ECM production and assembly. After sufficient culture time (e.g., ~5–7 days for a 3T3 mouse fibroblast cell line to yield a 10 μm thick ECM), the culture can be treated with 1% NP-40, or another mild detergent, to remove the cells but leave the insoluble ECM unperturbed (Figure 18.4c) [56]. In this protocol, unlike experiments using Matrigel, the original ECM structure remains intact and new cells can be seeded directly onto the vacant scaffold (Figure 18.4d).

Cell-derived matrices are generally soft (Young's moduli in the range of 10^0–10^2 Pa) [53, 61]. The stiffness of hydrogels formed from Matrigel can be

controlled by varying protein concentrations [62], although this has the unintended effect of also affecting ligand density and the concentration of soluble factors. Both Matrigel and decellularized ECMs can be stiffened using chemical cross-linkers, such as glutaraldehyde [23] or formaldehyde [63], although the degree of stiffening will depend on the composition and structure of the particular ECM. Despite the benefits of having a complex composition specifically made by your cells and eliciting some cell-behaviors absent on other substrates [64], these substrates suffer from substantial cell-type-to-cell-type and batch-to-batch variation, especially in the degree of cross-linking and thus the stiffness of the matrix. Most substrates are typically soft and can only be stiffened about threefold using chemical cross-linkers, some of which may be toxic above certain concentrations [53].

18.6 Synthetic Scaffolds

Although naturally derived materials may closely mimic the ECM *in vivo*, these natural materials often have a complexity and variability that make reductionist, material, and surface science-based studies of cell behavior difficult. An alternative to naturally derived polymers are synthetic polymer hydrogels, which may also be used as cell culture substrates. Three synthetic materials stand out in particular when considering surface mechanics regarding cell culture *in vitro*. Polyacrylamide (PA) [65], PEG, and polydimethylsiloxane (PDMS) [66–68] are well-defined materials in terms of both structure and mechanics [69, 70]. All three systems provide an extremely controllable and tunable alternative for natural materials when developing substrates with highly tunable yet precise stiffness [69]. Although these systems may lack biological epitopes to probe cell surface proteins, they can be modified such that their surfaces or internal structure present cell-appropriate ligands [3, 71].

18.6.1 Polyacrylamide Hydrogels

PA hydrogels are synthesized via radical polymerization of acrylamide subunits cross-linked with bis-acrylamide. Acrylamide chains are produced from the polymerization of acrylamide monomers, and these chains are cross-linked by bis-acrylamide [70, 72] (Figure 18.4e). Changing the relative concentrations of acrylamide to bis-acrylamide as well as changing the amount of initiator allows for variation of hydrogel elasticity. Increasing the relative ratio of bis-acrylamide to acrylamide increases cross-linking, which results in increased stiffness. Most commonly, TEMED and ammonium persulfate are used to trigger a free radical-dependent polymerization of vinyl groups in the acrylamide and bis-acrylamide monomers [72]. Alternatively, photoinitiators activated by exposure to ultraviolet (UV) light such as Irgacure or AIBN (azobisisobutyrnitrile) may be used instead when wanting to make spatial gradients of stiffness [2, 73]. The use of light diffusers or photomasks with photoinitiators can allow stiffness to be varied spatially [72].

With each of these changes, it is important to consider how surface mechanics are affected on the basis of the four metrics mentioned in Figure 18.3. For both PA and PEG systems, they will alter concentration and polymerization methods to create long chain entanglements or produce directly cross-linked hydrogels to modulate stiffness. Tse and Engler have directly shown how cross-link density and entanglement influence stiffness in PA hydrogels by direct measurement via AFM [65].

Although PA is inert and nonfouling, surfaces can be covalently functionalized with amine-containing peptides or proteins using several strategies. The most often employed is photoactivating the surface, making it amine-reactive via heterobifunctional cross-linkers, that is, a cross-linker that has a different reactive group on each end allowing for sequential reactions to occur [72]. Traditionally, a heterobifunctional cross-linker such as sulfo-SANPAH (sulfosuccinimidyl-6-(4′-azido-2′-nitrophenylamino) hexanoate) with a phenyl azide group on one end that can react with PA and a sulfosuccinimidyl group on the other end that can react with primary amines, is used to conjugate matrix proteins such as collagen or fibronectin onto the surface of the PA hydrogel [70, 72]. Carbodiimide-mediated cross-linking is another technique that is used to covalently attach proteins to PA hydrogels. EDC (1-ethyl-3-(3-dimethylaminopropyl)carbodiimide-HCL), a relatively inexpensive reagent, can react with a free carboxyl group to form an amine-reactive intermediate that reacts with amines on proteins for protein conjugation [72]. The free carboxyl group must be obtained by incorporating acrylic acid, the deamidation product of acrylamide, into the PA gel. Acrylic acid can then copolymerize along with acrylamide and bis-acrylamide. A third method of protein conjugation to PA hydrogels utilizes NHS-acrylate (*N*-hydroxysuccinimide ester), an acrylic acid with opposing NHS and acrylate groups. The acrylate group can copolymerize with acrylamide and bis-acrylamide, and the NHS group is reactive with amines in proteins. The NHS-acrylate can be concentrated to the surface by overlaying a solution of aqueous acrylamide and bis-acrylamide with a solution of immiscible toluene containing NHS-acrylate [72]. With this method, copolymerization of acrylamide with NHS-acrylate is restricted to the surface of the hydrogel. The addition of any amine will displace the NHS moiety and result in the covalent bonding of proteins to the hydrogel [72]. A variant of this method utilizes N6 (*N*-succinimidyl ester of acrylaminohexanoic acid) [72, 74]. Similarly to NHS-acrylate, one end group of N6 is incorporated into the PA gel and the *N*-succinimidyl ester on the other end is reactive to primary amines. N6 is not available commercially, and must be synthesized. First, acryloyl chloride is added to 6-aminohexanoic acid to yield 6-acrylamidohexanoic acid. EDC then catalyzes esterification with *N*-hydroxysuccinimide [72]. The resulting *N*-succinimidyl ester is treated with 6-aminohexanoic acid to yield 6-acrylamidohexylaminohexanoic acid, which is treated again with EDC to catalyze esterification with *N*-hydroxysuccinimide to yield N6 [72].

Despite its advantages as a culture substrate, including ease of use and linear elasticity over a wide range of elasticity, there are significant problems with PA that limit its applicability. A major drawback of acrylamide is its cytotoxic effects as a monomer [75]. Extensive washing is required to ensure that no monomer is present in the hydrogel before adding cells, and thus this material cannot be used

to encapsulate cells as is often the case with ECM *in vivo*. Therefore, cell culture using PA hydrogels must be limited to 2D studies *in vitro*. The pore size of the gel is near 100 nm, ensuring that cells will remain in 2D. As with HA, PA also has some variants that build in specific properties, such as the thermal reversibility of poly(*N*-isopropylacrylamide) (NIPAM) [76]. Upon crossing the lower critical solution temperature (LCST), NIPAM undergoes a reversible network collapse at 33 °C. However, this and other modifications provide properties that will be difficult to use in culture given their existence outside of conditions supportive of cell culture, for example, LCST well below normal culture temperature.

18.6.2 Poly(ethylene glycol)

PEG has been commonly used in biology owing to its resistance to protein adsorption. PEG is a relatively small monomer (Figure 18.4f) and does not polymerize itself, so it is typically conjugated to a group that does. Functionalized cross-linked PEG gels are synthesized by either chain or step growth polymerization depending on the polymerizable moieties that are incorporated to the PEG molecules [69, 77–79]. Chain photopolymerization of macromolecular PEG chains modified on either end with acrylate or methacrylate groups is the most common method of synthesizing PEG hydrogels. The resulting hydrogel structure is characterized by poly(meth)acrylate chains cross-linked with PEG. As PEG size and molecular weight vary, PEG hydrogels often cannot be characterized by traditional polymer science and polymer chemistry. Step growth polymerizations are an alternative to the chain polymerization PEG-di(meth)acrylate systems. The synthesis of PEG hydrogels through the reaction of comonomer solutions containing complementary reactive groups produces more homogeneous structures with less variation in mesh size [69]. These hydrogels may be synthesized using base-catalyzed Michael-type addition reactions between thiols and conjugated unsaturated functional groups and radical-mediated thiol-ene photopolymerizations [69].

In order to incorporate matrix peptide sequences, PEG is often conjugated to an acrylate on one end, and a peptide sequence such as arginine–glycine–aspartic acid (RGD), the minimum primary amino acid sequence in fibronectin required for binding to cell surface integrins, on the other end [80, 81]. The acrylated-PEG then can polymerize similarly to acrylamide; because the peptide sequence does not participate in polymerization, only one end of the molecule will participate in the polymerization reaction and be incorporated into the backbone of the gel. Similar to PA hydrogels, PEG hydrogels are also limited to 2D studies by their mesh size and cross-linking density, which make the material resistant to diffusion and protein adsorption as well as cellular migration in three dimensions. In order to enable cell–cell interactions or cellular migration, degradation of the material must be incorporated into the system [80].

18.6.3
Polydimethylsiloxane

PDMS is a viscoelastic polymer, composed of a silicone repeat unit (Figure 18.4g). To create a PDMS substrate, the monomer is mixed with a curing agent, degassed and incubated for several hours. The ratio of curing agent to monomer and the incubation time controls the stiffness of the substrate (between 10^4 and 10^6 Pa) [82]. The resulting PDMS is optically clear and nontoxic, but similar to other synthetic scaffolds, it must be modified to provide ligands for cell attachment. The strategies for functionalizing PDMS, similar to those for PA hydrogels, employ a heterobifunctional linker (e.g., Sulfo-SANPAH) to covalently link bioactive peptides or proteins to the substrate surface [70, 72]. The pore size of PDMS is thought to be in the nanometer range, too small for cells to migrate away from the substrate surface [83]. These properties make PDMS a useful substrate for studying cell behavior on two-dimensional surfaces of moderate to rigid stiffness. Importantly, a recent report has demonstrated differences in the way cells respond to PDMS and PA gels of the same stiffness, suggesting that there are potential differences between the ways cells interact with these two substrates, such as with how the matrix ligand is presented [66]. However, it should be noted that the study employs moduli outside the well-established range for PDMS [67, 68, 82], so it is not clear at the present time as to what caused the PDMS to appear so soft with Trapmann and coworkers [66].

Once polymerized, PDMS maintains its shape with high fidelity, making it useful for applications where precise spatial or topographic control is required, such as in the creation of micropillar substrates [84] and microfluidic devices [83]. Cells seeded onto a surface of micropillars exert traction forces onto the pillars, causing them to bend. By monitoring the displacement of the pillars, the magnitude of a cell's traction forces may be calculated in real time [84]. Microfluidic devices composed of PDMS are commonly used to create smooth gradients of one or more soluble molecules. This can be used to study the response of a cell type to a chemical factor at a range of concentrations or, by varying the concentration of bisacrylamide, to create a PA gel with a defined stiffness gradient.

18.7
Substrate Stiffness' Impact on Cell Behavior

Most cell types plated on soft, for example, 1 kPa hydrogels, or stiff substrates, for example, Petri dishes, exhibit dramatically different behavior. While cells spread out on stiff substrates, cells on soft substrates have a round morphology, that is, circularity closer to 1 or a perfect circle, and will have smaller spread areas. While some cell types such as neurons exhibit phenotypic behavior on softer substrates [85], most cell types display substrate stiffness-dependent morphological and functional changes. For example, proliferation is generally positively regulated by matrix stiffness [20]; proliferation rates on soft substrates are lower than on

stiff substrates. Substrate stiffness has the ability to regulate cell survival [86], motility [87], and differentiation [4]. Most of these experiments were performed in 2D, but selected studies that have extended substrate stiffness control to 3D have seen differences [56, 88]. Thus when assessing stiffness-dependent behavior, it is important to note that matrix dimensionality as well as porosity may have an effect on cell behavior [33]. This section focuses on cell responses to matrix stiffness *in vitro* and provides a brief discussion of mechanotransduction – the mechanism that allows cells to ''feel'' stiffness.

Stiffness-dependent behavior was first characterized in differentiated cells that naturally want to reside in a niche that mimics its native environment. Muscle, for example, resides in an ECM-rich niche approximately 5–20 kPa depending on the species and muscle type (Figure 18.1b) [21, 32]; skeletal muscle cells in such niche form striated muscle only within this tight range [14, 89]. Smooth muscle also exhibits phenotypic behavior [90–92] and remains contractile [93] in conditions that resemble smooth muscle stiffness [14]. Cancer, while not having a ''lineage'' *per se*, does exhibit invasive behavior at specific stiffness [40], which will be detailed subsequently. Adult stem cells have the unique state where no specific lineage is preferred, but when presented with a matrix of a given set of properties, they can use these properties as cues for differentiation. For example, during wound healing, adult stem cells are recruited to the site of injury in order to help create new tissue, and at this site, matrix stiffness is thought to play a major role in recruiting and guiding the fate of these cells. Mesenchymal stem cells (MSCs) have been shown to differentiate into various anchorage-dependent cell types including neurons, myoblasts, and osteoblasts, induced by soluble chemical stimuli as well as matrix elasticity [4, 94]. More specifically, when human MSCs were plated on collagen-coated PA gels, with stiffnesses of 0.1–1 kPa (''brain''), 8–17 kPa (''muscle''), and 25–40 kPa (''bone''), the morphology, transcriptional profile, and expression of marker proteins resembled those of the compliant substrate after 1 week. MSCs grown on the softest substrates resembled those of cultured neurons, MSCs on the medium stiffness substrates resembled myoblasts, and MSCs grown on the stiff substrate resembled osteoblasts. Not only was this lineage commitment guided solely by matrix stiffness, but it can also be proposed that matrix stiffness is in fact more important than the soluble factors. MSCs committed to the matrix-derived lineage even if opposing signals from opposing soluble markers were present, but this occurred in a time-dependent manner; early in the culture, cell phenotype was ''plastic,'' meaning that substrate and chemical cues could regulate fate but after weeks in culture, phenotype had been established. These data have been confirmed using matrix with dynamic properties, which enable one to stiffen the matrix over time [95]. This data suggests that matrix elasticity plays an extremely important and possibly dominating role in specifying stem cell lineage as it modified cells' ability to interact with growth factors, serum, and so on.

It is currently uncertain how cells actually gather information about matrix stiffness and translate that into a cellular response. In other words, how do cells convert mechanical stimuli into biochemical signals? Two main classes of mechanotransduction have been proposed, that is, nuclear and peri-membranous,

as the result of either passive (outside-in) or active (inside-out) signaling. For passive (outside-in) signaling, cells respond to external forces, including shear stress, extension, compression, and pressure, while active (inside-out) sensing involves cells probing or measuring the mechanical properties of their extracellular environment. While beyond the scope here, a good overview of active versus passive mechanotransduction can be found elsewhere [96, 97]. What we focus here on, however, is the location and method of sensing. In nuclear-mediated mechanisms, forces transmitted to the nucleus result in deformation/stretching that pulls on the chromosomes [98], changing their accessibility or deacetylating specific regions [99, 100]. For sensing occurring at and around the cell membrane, several mechanosignaling methods have been proposed and include Rho/ROCK signaling [70, 91], stretch activated channels [101], and mechanical strain gauges [102]. Briefly, Rho/ROCK signaling includes the force-induced upregulation of contractile proteins which positively feedback on Rho signaling to further enhance contractility [103]. Stretch activated channels, which are critically important for muscle function, differentially control ion concentration to regulate cells' ability to contract and ''feel'' their niche. Molecular strain gauges use force-induced conformational changes in proteins to alter accessibility to binding sites that could convert biophysical to biochemical cues [96]. Each of these has specific differences that are covered elsewhere [96].

18.8 When Stiffness *In vivo* Goes Awry: The Impact of Fibrosis on Function

Fibrosis, the accumulation of excess and abnormal ECM often occurring during wound healing [104], is the major disease model of altering tissue stiffness *in vivo* motivating the study of substrate stiffness *in vitro*. While replacing injured tissue with normal healthy tissue is ideal, most often the wound healing process goes awry [105, 106] as injured tissue is gradually replaced with fibrous connective tissue, resulting in scar formation that is different in composition and several-fold stiffer than healthy tissue [104, 107]. In addition to increased matrix production, fibrosis can also occur through decreased matrix degradation [105, 108, 109]. Fibrosis may occur in many tissues, including the bone marrow (myelofibrosis) [110], lungs (pulmonary fibrosis) [111], liver (cirrhosis) [105], intestines (Crohn's disease) [112], and heart (endomyocardial fibrosis and myocardial infarct) [113]. This final section of the chapter focuses on liver fibrosis as a case study, which, as shown in Figure 18.1b, has significantly elevated stiffness from a normal liver, and describes how specific aspects of the disease, that is, stiffness, can be mimicked *in vitro*.

Liver fibrosis arises from the wound healing response to chronic liver damage that may result from viral hepatitis, ethanol abuse, biliary obstruction, autoimmune disorders, or metabolic diseases [104, 105, 114, 115]. In 2003, over 900 000 patients suffered from cirrhosis, the end stage of liver disease or liver injury characterized by untreatable fibrosis [114, 115]. Viral hepatitis, specifically hepatitis B and hepatitis C, is the leading risk factor of liver fibrosis globally, while liver disease stemming from alcoholism is the leading risk factor of liver fibrosis in developed nations [116, 117].

The primary characteristic of liver fibrosis is the accumulation of up to sixfold more ECM including fibrillar collagens, fibronectin, and proteoglycans [104, 116, 118]. The additional matrix, deposited by α-smooth muscle actin expressing contractile myofibroblasts [104, 109], causes a near threefold stiffening of the tissue [104]. Hepatic stellate cells found in the liver are activated during fibrosis, then migrate and accumulate at sites of tissue repair [109], and transdifferentiate into myofibroblasts [104, 119]. In culture, hepatic stellate cells transdifferentiate into myofibroblasts in response to increased substrate stiffness [104, 120], indicating stiffness-induced positive feedback. During fibrosis however, tissue stiffness increases before myofibroblasts are activated and before excess matrix is produced and deposited in the liver [104].

The initial increase in tissue stiffness immediately after the onset of fibrosis may be attributed to increases in lysyl oxidase activity [104, 121–123]. Lysyl oxidase catalyzes the formation of highly reactive aldehydes from lysine residues in collagen [124] to form cross-linked collagen that can increase matrix stiffness [125]. Lysyl oxidase activity in a fibrotic liver is four to sixfold greater than in a normal healthy liver [124]. The initial stiffness increase has been shown to activate hepatic stellate cells to transdifferentiate into myofibroblasts, which deposit excess matrix, increasing tissue stiffness, and further activates even more hepatic stellate cells to transdifferentiate [124]. However, the accumulation of matrix is also an effect of decreased matrix degradation [116, 126]. As excess collagen is deposited, the simultaneous increase in cross-linking activity protects the newly deposited collagen from being degraded or remodeled by collagenase [127, 128], further prompting this increasing tissue stiffness positive feedback mechanism. In normal matrix remodeling, metalloproteinases (matrix metalloproteinases, MMPs) degrade various matrix proteins. Decreased degradation in fibrosis is also attributed to increased secretion of MMP inhibitors [108, 109]. What results is a soft matrix of approximately 600 Pa that stiffens threefold over a month [104]. Using the materials mentioned here, such temporal changes can be easily mimicked *in vitro*.

18.9 Novel Surface Fabrication Techniques to Improve Biomimicry

Cell behavior *in vitro* most closely resembles *in vivo* cell behavior when cells are grown on substrates that mimic the stiffness of their native environment [32, 55]. However, the ECM is not static. As a result, there is a significant need for biomimetic hydrogels to have dynamically tunable properties that can probe and respond to complex cellular behavior [69]. Recent dynamic hydrogels, where stiffness may change either spatially or temporally, represent the newest area of exploration.

Physiological spatial gradients of tissue stiffness may be observed within a tissue, as well as at tissue interfaces [65]. For example, cells *in vivo* may encounter physiological stiffness gradients such as the bone (stiff)–cartilage (soft) interface [3, 4, 129]. Pathological stiffness gradients on the other hand may arise during wound

healing; a myocardium postinfarction forms a fibrotic scar that is several-fold stiffer than healthy tissue [3, 107]. In either case, migrating cells such as MSCs that travel from their source to a specific tissue where they then differentiate, will encounter stiffness gradients and thus will feel changes in environmental stiffness along the way. PA gels that vary in stiffness spatially have been created to study stem cell durotaxis, or the migration of cells solely due to changes in stiffness, *in vitro*. Gradient photomasks that filter UV light to create a gradient of UV intensity and a photoinitiator, such as Irgacure, can be used to fabricate PA gels with shallow stiffness gradients [65, 130]. Microfluidic gradient generators allowing for greater stiffness control have also been developed in order to create somewhat steeper PA stiffness gradients [2, 73]. Although biomimetic gradients of collagen or other matrix protein may also be used to fabricate a 3D biological stiffness gradient gel *in vitro* [131], it is important to note that these systems do not effectively decouple ligand and stiffness gradients.

Tissue stiffness also varies temporally. Chicken heart, for example, develops from soft mesoderm tissue with a stiffness that is less than 0.5 kPa, and stiffens as development progresses up to 10 kPa over the course of several weeks [55, 132]. Thiolated HA gels, which undergo a Michael-type reaction with PEG diacrylate of varying molecular weight, can stiffen in a similar manner as previously mentioned. This time-stiffening material mimicking developmental stiffening has been shown to improve cardiomyocyte maturation and sarcomere assembly [55]. Collagen-alginate hydrogels, which are cross-linked using divalent cations such as calcium, can also have temporally changing stiffness as step changes in calcium-induced cross-linking can be titrated into the network. However, this process requires adding calcium externally, over time, which may alter cell signaling [133]. pH and temperature changes have also been proposed to modulate network elasticity [134, 135], but these change niche hydrophobicity and may potentially alter cell metabolism from prolonged culture in less-than-optimal media conditions. Using principles similar to thiolated HA hydrogel stiffening, Guvendiren and Burdick have recently described how a methacrylated HA hydrogel, which uses dithiothreitol (DTT) to initially cross-link the hydrogel, subsequently has time-dependent cross-linking with stepwise activation via UV-activated, free radical polymerization [50].

18.10 Conclusion

The current state of stiffness-altering materials is transitioning from 2D to 3D, and from synthetic materials to more biomimetic natural biological materials. Cells reside in 3D *in vivo*, and dimensionality has shown to significantly affect cell adhesion, migration, and gene expression [136]. The incorporation of varying stiffness in 3D, both temporally and spatially, will allow for the understanding of tissue development and tissue wound healing, both of which provide a foundation for the investigation of tissue engineering therapies.

Acknowledgment

The authors would like to thank Jennifer L. Young for kindly providing the image used in Figure 18.4a. The authors would also like to thank NIH for providing funding for this effort (DP02OD006460 and R21EB011727 to A.J.E.).

Abbreviations

Pa	Pascals
ECM	extracellular matrix
AFM	atomic force microscopy
HA	hyaluronic acid
PEG	polyethylene glycol
PA	polyacrylamide
UV	ultraviolet
PDMS	polydimethylsiloxane

References

1. Isenberg, B.C., Dimilla, P.A., Walker, M., Kim, S., and Wong, J.Y. (2009) *Biophys. J.*, **97**, 1313–1322.
2. Zaari, N., Rajagopalan, P., Kim, S.K., Engler, A.J., and Wong, J.Y. (2004) *Adv. Mater.*, **16**, 2133–2137.
3. Tse, J.R. and Engler, A.J. (2011) *PLoS ONE*, **6**, e15978.
4. Engler, A.J., Sen, S., Sweeney, H.L., and Discher, D.E. (2006) *Cell*, **126**, 677–689.
5. Turner, C.H., Rho, J., Takano, Y., Tsui, T.Y., and Pharr, G.M. (1999) *J. Biomech.*, **32**, 437–441.
6. Fung, Y. (1993) *Biomechanics: Mechanical Properties of Living Tissues*, Vol. 12, Springer, New York.
7. Treloar, L.R.G. (2005) *The Physics of Rubber Elasticity*, Oxford University Press, New York.
8. Gibson, L.J., Easterling, K.E., and Ashby, M.F. (1981) *Proc. R. Soc. London, Ser. A*, **377**, 99–117.
9. David, M.W. and Engler, A.J. (2010) *J. Biomech.*, **43**, 1.
10. Flores-Merino, M.V., Chirasatitsin, S., Lopresti, C., Reilly, G.C., Battaglia, G., and Engler, A.J. (2010) *Soft Matter*, **6**, 4466–4470.
11. Lu, H.D., Charati, M.B., Kim, I.L., and Burdick, J.A. (2012) *Biomaterials*, **33**, 2145–2153.
12. Storm, C., Pastore, J., MacKintosh, F., and Lubensky, T. (2005) *Nature*, **435**, 191–194.
13. Jacot, J.G., Dianis, S., Schnall, J., and Wong, J.Y. (2006) *J. Biomed. Mater. Res. A*, **79**, 485–494.
14. Engler, A.J., Richert, L., Wong, J.Y., Picart, C., and Discher, D.E. (2004) *Surf. Sci.*, **570**, 142–154.
15. Dimitriadis, E. (2002) *Biophys. J.*, **82**, 2798–2810.
16. Lin, D.C., Dimitriadis, E.K., and Horkay, F. (2007) *J. Biomech. Eng.*, **129**, 430–440.
17. Fabry, B., Maksym, G., Butler, J., Glogauer, M., Navajas, D., and Fredberg, J. (2001) *Phys. Rev. Lett.*, **87**, 1–4.
18. Kasza, K.E., Nakamura, F., Hu, S., Kollmannsberger, P., Bonakdar, N., Fabry, B., Stossel, T.P., Wang, N., and Weitz, D.A. (2009) *Biophys. J.*, **96**, 4326–4335.
19. Ferry, J.D. (1980) *Viscoelastic Properties of Polymers*, John Wiley & Sons, Inc., New York.

20. Wells, R.G. (2008) *Hepatology (Baltimore)*, **47**, 1394–1400.
21. Discher, D.E., Janmey, P., and Wang, Y.-L. (2005) *Science (New York)*, **310**, 1139–1143.
22. Flory, P. (1953) *Principles of Polymer Chemistry*, Cornell University Press, Ithaca, NY.
23. Soucy, P.A. and Romer, L.H. (2009) *Matrix Biol.*, **28**, 273–283.
24. Callister, W. and Rethwisch, D. (2010) *Materials Science and Engineering: An Introduction*, 8th edn, John Wiley & Sons, Inc., Hoboken, NJ.
25. Zhang, X., Reagan, M.R., and Kaplan, D.L. (2009) *Adv. Drug Deliv. Rev.*, **61**, 988–1006.
26. Pariente, J.L., Kim, B.S., and Atala, A. (2002) *J. Urol.*, **167**, 1867–1871.
27. Hodde, J. (2002) *Tissue Eng.*, **8**, 295–308.
28. Singelyn, J.M. and Christman, K.L. (2010) *J. Cardiovasc. Transl. Res.*, **3**, 478–486.
29. Hay, E. (1991) *Cell Biology of Extracellular Matrix*, Plenum Press, New York.
30. Badylak, S.F., Freytes, D.O., and Gilbert, T.W. (2009) *Acta Biomater.*, **5**, 1–13.
31. Ott, H.C., Matthiesen, T.S., Goh, S.-K., Black, L.D., Kren, S.M., Netoff, T.I., and Taylor, D.A. (2008) *Nat. Med.*, **14**, 213–221.
32. Discher, D.E., Mooney, D.J., and Zandstra, P.W. (2009) *Science (New York)*, **324**, 1673–1677.
33. Reilly, G.C. and Engler, A.J. (2010) *J. Biomech.*, **43**, 55–62.
34. Fratzl, P. (2008) *Collagen: Structure and Mechanics*, Springer Science+Business Media, New York.
35. Myllyharju, J. and Kivirikko, K.I. (2004) *Trends Genet.*, **20**, 33–43.
36. Huxley-Jones, J., Robertson, D.L., and Boot-Handford, R.P. (2007) *Matrix Biol.*, **26**, 2–11.
37. Girton, T., Oegema, T., Grassl, E., Isenberg, B., and Tranquillo, R. (2000) *J. Biomech. Eng.*, **122**, 216–223.
38. Knott, L. and Bailey, A.J. (1998) *Bone*, **22**, 181–187.
39. Levental, K.R., Yu, H., Kass, L., Lakins, J.N., Egeblad, M., Erler, J.T., Fong, S.F.T., Csiszar, K., Giaccia, A., Weninger, W., Yamauchi, M., Gasser, D.L., and Weaver, V.M. (2009) *Cell*, **139**, 891–906.
40. Paszek, M.J., Zahir, N., Johnson, K.R., Lakins, J.N., Rozenberg, G.I., Gefen, A., Reinhart-King, C.A., Margulies, S.S., Dembo, M., Boettiger, D., Hammer, D.A., and Weaver, V.M. (2005) *Cancer Cell*, **8**, 241–254.
41. Achilli, M. and Mantovani, D. (2010) *Polymers*, **2**, 664–680.
42. Sundararaghavan, H.G., Monteiro, G.A., Lapin, N.A., Chabal, Y.J., Miksan, J.R., and Shreiber, D.I. (2008) *J. Biomed. Mater. Res. A*, **87**, 308–320.
43. Engler, A., Bacakova, L., Newman, C., Hategan, A., Griffin, M., and Discher, D. (2004) *Biophys. J.*, **86**, 617–628.
44. Ulrich, T.A., Jain, A., Tanner, K., MacKay, J.L., and Kumar, S. (2010) *Biomaterials*, **31**, 1875–1884.
45. Tierney, C.M., Haugh, M.G., Liedl, J., Mulcahy, F., Hayes, B., and O'Brien, F.J. (2009) *J. Mech. Behav. Biomed. Mater.*, **2**, 202–209.
46. Varki, A., Cummings, R., Esko, J., Freeze, H., Hart, G., and Marth, J. (1999) *Essentials of Glycobiology*, Cold Spring Harbor Laboratory Press, Cold Spring Harbor, NY.
47. Burdick, J.A. and Prestwich, G.D. (2011) *Adv. Mater. (Deerfield Beach)*, **23**, H41–H56.
48. Lesley, J., Hascall, V.C., Tammi, M., and Hyman, R. (2000) *J. Biol. Chem.*, **275**, 26967–26975.
49. Shu, X.Z., Liu, Y., Luo, Y., Roberts, M.C., and Prestwich, G.D. (2002) *Biomacromolecules*, **3**, 1304–1311.
50. Guvendiren, M. and Burdick, J.A. (2012) *Nat. Commun.*, **3**, 792.
51. Ananthanarayanan, B., Kim, Y., and Kumar, S. (2011) *Biomaterials*, **32**, 7913–7923.
52. Vanderhooft, J.L., Alcoutlabi, M., Magda, J.J., and Prestwich, G.D. (2009) *Macromol. Biosci.*, **9**, 20–28.
53. Soucy, P.A., Werbin, J., Heinz, W., Hoh, J.H., and Romer, L.H. (2011) *Acta Biomater.*, **7**, 96–105.
54. Kloxin, A.M., Kasko, A.M., Salinas, C.N., and Anseth, K.S. (2009) *Science (New York)*, **324**, 59–63.

55. Young, J.L. and Engler, A.J. (2011) *Biomaterials*, **32**, 1002–1009.
56. Cukierman, E., Pankov, R., Stevens, D.R., and Yamada, K.M. (2001) *Science (New York)*, **294**, 1708–1712.
57. Kleinman, H.K. and Martin, G.R. (2005) *Semin. Cancer Biol.*, **15**, 378–386.
58. Goffin, J.M., Pittet, P., Csucs, G., Lussi, J.W., Meister, J.-J., and Hinz, B. (2006) *J. Cell Biol.*, **172**, 259–268.
59. Vukicervic, S., Kleinman, H., Luyten, F., Roberts, A., Roche, N., and Reddi, A. (1992) *Exp. Cell Res.*, **202**, 1–8.
60. Singelyn, J.M., DeQuach, J.A., Seif-Naraghi, S.B., Littlefield, R.B., Schup-Magoffin, P.J., and Christman, K.L. (2009) *Biomaterials*, **30**, 5409–5416.
61. Soofi, S.S., Last, J.A., Liliensiek, S.J., Nealey, P.F., and Murphy, C.J. (2009) *J. Struct. Biol.*, **167**, 216–219.
62. Zaman, M.H., Trapani, L.M., Sieminski, A.L., Siemeski, A., Mackellar, D., Gong, H., Kamm, R.D., Wells, A., Lauffenburger, D.A., and Matsudaira, P. (2006) *Proc. Natl. Acad. Sci. U.S.A.*, **103**, 10889–10894.
63. Kubow, K.E., Klotzsch, E., Smith, M.L., Gourdon, D., Little, W.C., and Vogel, V. (2009) *Integr. Biol.*, **1**, 635–648.
64. Petrie, R.J., Gavara, N., Chadwick, R.S., and Yamada, K.M. (2012) *J. Cell Biol.*, **197**, 439–455.
65. Tse, J.R. and Engler, A.J. (2010) *Curr. Protoc. Cell Biol.*, **47**, 10.16.1–10.16.16(editorial board, Juan S. Bonifacino ... [et al.]).
66. Trappmann, B., Gautrot, J., and Connelly, J. (2012) *Nat. Mater.*, **11**, 642–649.
67. Kaushik, G., Fuhrmann, A., Cammarato, A., and Engler, A.J. (2011) *Biophys. J.*, **101**, 2629–2637.
68. Fu, J., Wang, Y.-K., Yang, M.T., Desai, R.A., Yu, X., Liu, Z., and Chen, C.S. (2010) *Nat. Methods*, **7**, 733–736.
69. Kloxin, A.M., Kloxin, C.J., Bowman, C.N., and Anseth, K.S. (2010) *Adv. Mater. (Deerfield Beach)*, **22**, 3484–3494.
70. Pelham, R.J. (1997) *Proc. Natl. Acad. Sci. U.S.A.*, **94**, 13661–13665.
71. Lutolf, M.P., Gilbert, P.M., and Blau, H.M. (2009) *Nature*, **462**, 433–441.
72. Kandow, C.E., Georges, P.C., Janmey, P.A., and Beningo, K.A. (2007) *Methods Cell Biol.*, **83**, 29–46.
73. Burdick, J.A., Khademhosseini, A., and Langer, R. (2004) *Langmuir*, **20**, 5153–5156.
74. Reinhart-King, C.A., Dembo, M., and Hammer, D.A. (2005) *Biophys. J.*, **89**, 676–689.
75. Besaratinia, A. and Pfeifer, G.P. (2003) *J. Natl. Cancer Inst.*, **95**, 889–896.
76. Convertine, A.J., Lokitz, B.S., Vasileva, Y., Myrick, L.J., Scales, C.W., Lowe, A.B., and McCormick, C.L. (2006) *Macromolecules*, **39**, 1724–1730.
77. Cruise, G.M., Scharp, D.S., and Hubbell, J.A. (1998) *Biomaterials*, **19**, 1287–1294.
78. Hern, D.L. and Hubbell, J.A. (1998) *J. Biomed. Mater. Res.*, **39**, 266–276.
79. Raeber, G.P., Lutolf, M.P., and Hubbell, J.A. (2005) *Biophys. J.*, **89**, 1374–1388.
80. Karpiak, J.V., Ner, Y., and Almutairi, A. (2012) *Adv. Mater. (Deerfield Beach)*, **24**, 1466–1470.
81. Miller, J.S., Shen, C.J., Legant, W.R., Baranski, J.D., Blakely, B.L., and Chen, C.S. (2010) *Biomaterials*, **31**, 3736–3743.
82. Gray, D.S., Tien, J., and Chen, C.S. (2003) *J. Biomed. Mater. Res. A*, **66A**, 605–614.
83. Yuen, P.K., Su, H., Goral, V.N., and Fink, K.A. (2011) *Lab Chip*, **11**, 1541–1544.
84. Saez, A., Buguin, A., Silberzan, P., and Ladoux, B. (2005) *Biophys. J.*, **89**, L52–L54.
85. Georges, P.C., Miller, W.J., Meaney, D.F., Sawyer, E.S., and Janmey, P.A. (2006) *Biophys. J.*, **90**, 3012–3018.
86. Wang, H.B., Dembo, M., and Wang, Y.L. (2000) *Am. J. Physiol. Cell Physiol.*, **279**, C1345–C1350.
87. Guo, W., Frey, M.T., Burnham, N.A., and Wang, Y.-L. (2006) *Biophys. J.*, **90**, 2213–2220.
88. Huebsch, N., Arany, P.R., Mao, A.S., Shvartsman, D., Ali, O.A., Bencherif, S.A., Rivera-Feliciano, J., and Mooney, D.J. (2010) *Nat. Mater.*, **9**, 518–526.
89. Collinsworth, A.M., Zhang, S., Kraus, W.E., and Truskey, G.A. (2002)

Am. J. Physiol. Cell Physiol., **283**, C1219–C1227.
90. Griffin, M.A., Engler, A.J., Barber, T.A., Healy, K.E., Sweeney, H.L., and Discher, D.E. (2004) *Biophys. J.*, **86**, 1209–1222.
91. Peyton, S.R. and Putnam, A.J. (2005) *J. Cell. Physiol.*, **204**, 198–209.
92. Wong, J.Y., Velasco, A., Rajagopalan, P., and Pham, Q. (2003) *Langmuir*, **19**, 1908–1913.
93. Wang, N., Tolić-Nørrelykke, I.M., Chen, J., Mijailovich, S.M., Butler, J.P., Fredberg, J.J., and Stamenović, D. (2002) *Am. J. Physiol. Cell Physiol.*, **282**, C606–C616.
94. Rowlands, A.S., George, P.A., and Cooper-White, J.J. (2008) *Am. J. Physiol. Cell Physiol.*, **295**, C1037–C1044.
95. Guvendiren, M. and Burdick, J.A. (2010) *Biomaterials*, **31**, 6511–6518.
96. Holle, A.W. and Engler, A.J. (2011) *Curr. Opin. Biotechnol.*, **22**, 648–654.
97. Jaalouk, D.E. and Lammerding, J. (2009) *Nat. Rev. Mol. Cell Biol.*, **10**, 63–73.
98. Dahl, K.N., Ribeiro, A.J.S., and Lammerding, J. (2008) *Circ. Res.*, **102**, 1307–1318.
99. Li, Y., Chu, J.S., Kurpinski, K., Li, X., Bautista, D.M., Yang, L., Sung, K.-L.P., and Li, S. (2011) *Biophys. J.*, **100**, 1902–1909.
100. Poh, Y.C., Shevtsov, S.P., Chowdhury, F., Wu, D.C., Na, S., Dundr, M., and Wang, N. (2012) *Nat. Commun.*, **3**, 866.
101. Christensen, O. (1987) *Nature*, **330**, 66–68.
102. Duncan, R.L. and Turner, C.H. (1995) *Calcif. Tissue Int.*, **57**, 344–358.
103. Lo, C.M., Wang, H.B., Dembo, M., and Wang, Y.L. (2000) *Biophys. J.*, **79**, 144–152.
104. Georges, P.C., Hui, J.-J., Gombos, Z., McCormick, M.E., Wang, A.Y., Uemura, M., Mick, R., Janmey, P.A., Furth, E.E., and Wells, R.G. (2007) *Am. J. Physiol. Gastrointest. Liver Physiol.*, **293**, G1147–G1154.
105. Wells, R.G. (2005) *J. Clin. Gastroenterol.*, **39**, S158–S161.
106. Border, W.A. and Noble, N.A. (1994) *N. Engl. J. Med.*, **331**, 1286–1292.
107. Berry, M.F., Engler, A.J., Woo, Y.J., Pirolli, T.J., Bish, L.T., Jayasankar, V., Morine, K.J., Gardner, T.J., Discher, D.E., and Sweeney, H.L. (2006) *Am. J. Physiol. Heart Circ. Physiol.*, **290**, H2196–H2203.
108. Arthur, M.J. (2000) *Am. J. Physiol. Gastrointest. Liver Physiol.*, **279**, G245–G249.
109. Bataller, R. and Brenner, D.A. (2005) *J. Clin. Invest.*, **115**, 209–218.
110. Tefferi, A. (2011) *Am. J. Hematol.*, **86**, 1017–1026.
111. Dancer, R.C.A., Wood, A.M., and Thickett, D.R. (2011) *Eur. Respir. J.*, **38**, 1461–1467.
112. Spinelli, A., Correale, C., Szabo, H., and Montorsi, M. (2010) *Curr. Drug Targets*, **11**, 242–248.
113. Burlew, B.S. and Weber, K.T. (2002) *Herz*, **27**, 92–98.
114. Wang, M.H., Palmeri, M.L., Guy, C.D., Yang, L., Hedlund, L.W., Diehl, A.M., and Nightingale, K.R. (2009) *Ultrasound Med. Biol.*, **35**, 1709–1721.
115. Friedman, S.L. (2003) *J. Hepatol.*, **38** (Suppl. 1), S38–S53.
116. Thompson, K.J., McKillop, I.H., and Schrum, L.W. (2011) *World J. Gastroenterol.*, **17**, 2473–2481.
117. Rombouts, K. and Marra, F. (2010) *Dig. Dis. (Basel)*, **28**, 229–235.
118. Imai, K., Sato, T., and Senoo, H. (2000) *Cell Struct. Funct.*, **25**, 329–336.
119. Guyot, C., Lepreux, S., Combe, C., Doudnikoff, E., Bioulac-Sage, P., Balabaud, C., and Desmoulière, A. (2006) *Int. J. Biochem. Cell Biol.*, **38**, 135–151.
120. Li, Z., Dranoff, J.A., Chan, E.P., Uemura, M., Sévigny, J., and Wells, R.G. (2007) *Hepatology (Baltimore)*, **46**, 1246–1256.
121. Brüel, A., Ortoft, G., and Oxlund, H. (1998) *Atherosclerosis*, **140**, 135–145.
122. Elbjeirami, W.M., Yonter, E.O., Starcher, B.C., and West, J.L. (2003) *J. Biomed. Mater. Res. A*, **66**, 513–521.
123. Norton, G.R., Tsotetsi, J., Trifunovic, B., Hartford, C., Candy, G.P., and Woodiwiss, A.J. (1997) *Circulation*, **96**, 1991–1998.

124. Wakasaki, H. and Ooshima, A. (1990) *Biochem. Biophys. Res. Commun.*, **166**, 1201–1204.

125. Huang, D., Chang, T.R., Aggarwal, A., Lee, R.C., and Ehrlich, H.P. (1993) *Ann. Biomed. Eng.*, **21**, 289–305.

126. Wynn, T.A. (2008) *J. Pathol.*, **214**, 199–210.

127. Mormone, E., George, J., and Nieto, N. (2011) *Chem. Biol. Interact.*, **193**, 225–231.

128. Han, Y.-P., Zhou, L., Wang, J., Xiong, S., Garner, W.L., French, S.W., and Tsukamoto, H. (2004) *J. Biol. Chem.*, **279**, 4820–4828.

129. Guilak, F. (2000) *Biorheology*, **37**, 27–44.

130. Marklein, R.A. and Burdick, J.A. (2010) *Soft Matter*, **6**, 136.

131. Hadjipanayi, E., Mudera, V., and Brown, R.A. (2009) *Cell Motil. Cytoskeleton*, **66**, 121–128.

132. Hamburger, V. and Hamilton, H.L. (1992) *Dev. Dyn.*, **195**, 231–272.

133. Gillette, B.M., Jensen, J.A., Wang, M., Tchao, J., and Sia, S.K. (2010) *Adv. Mater. (Deerfield Beach)*, **22**, 686–691.

134. Yamato, M., Utsumi, M., Kushida, A., Konno, C., Kikuchi, A., and Okano, T. (2001) *Tissue Eng.*, **7**, 473–480.

135. Yoshikawa, H.Y., Rossetti, F.F., Kaufmann, S., Kaindl, T., Madsen, J., Engel, U., Lewis, A.L., Armes, S.P., and Tanaka, M. (2011) *J. Am. Chem. Soc.*, **133**, 1367–1374.

136. Pampaloni, F., Reynaud, E.G., and Stelzer, E.H.K. (2007) *Nat. Rev. Mol. Cell Biol.*, **8**, 839–845.